Developmental Cell, Vol. 3, 593–603, October, 2002, Copyright ©2002 by Cell Press

Pseudomonas aeruginosa Anaerobic Respiration in Biofilms: Relationships to Cystic Fibrosis Pathogenesis

Sang Sun Yoon,[1] Robert F. Hennigan,[2] George M. Hilliard,[3] Urs A. Ochsner,[4] Kislay Parvatiyar,[1] Moneesha C. Kamani,[1] Holly L. Allen,[1] Teresa R. DeKievit,[5] Paul R. Gardner,[6] Ute Schwab,[7] John J. Rowe,[8] Barbara H. Iglewski,[9] Timothy R. McDermott,[10] Ronald P. Mason,[11] Daniel J. Wozniak,[12] Robert E.W. Hancock,[13] Matthew R. Parsek,[14] Terry L. Noah,[7] Richard C. Boucher,[7] and Daniel J. Hassett[1,15]

[1]Departments of Molecular Genetics, Biochemistry and Microbiology,
[2]Cell Biology, and
[3]Molecular and Cellular Physiology
University of Cincinnati College of Medicine
Cincinnati, Ohio 45267
[4]Department of Microbiology
University of Colorado Health Sciences
Denver, Colorado 80262
[5]Department of Microbiology and Immunology
University of Manitoba
Winnipeg, Manitoba R3T 2N2
Canada
[6]Division of Critical Care Medicine
Children's Hospital Medical Center
Cincinnati, Ohio 45229
[7]Department of Pulmonary Biology
University of North Carolina
Chapel Hill, North Carolina 27599
[8]Department of Biology
University of Dayton
Dayton, Ohio 45469
[9]Department of Microbiology and Immunology
University of Rochester
Rochester, New York 14642
[10]Department of Land Resources
Montana State University
Bozeman, Montana 59717
[11]Laboratory of Pharmacology and Chemistry
NIEHS
Research Triangle Park, North Carolina 27709
[12]Department of Microbiology and Immunology
Wake Forest University School of Medicine
Winston-Salem, North Carolina 27157
[13]Department of Microbiology and Immunology
University of British Columbia
Vancouver, British Columbia VT6 1Z3
Canada
[14]Department of Civil Engineering
Northwestern University
Evanston, Illinois 60208

Summary

Recent data indicate that cystic fibrosis (CF) airway mucus is anaerobic. This suggests that *Pseudomonas aeruginosa* infection in CF reflects biofilm formation and persistence in an anaerobic environment. *P. aeruginosa* formed robust anaerobic biofilms, the viability of which requires *rhl* quorum sensing and nitric oxide (NO) reductase to modulate or prevent accumulation of toxic NO, a byproduct of anaerobic respiration. Proteomic analyses identified an outer membrane protein, OprF, that was upregulated ~40-fold under anaerobic versus aerobic conditions. Further, OprF exists in CF mucus, and CF patients raise antisera to OprF. An *oprF* mutant formed poor anaerobic biofilms, due, in part, to defects in anaerobic respiration. Thus, future investigations of CF pathogenesis and therapy should include a better understanding of anaerobic metabolism and biofilm development by *P. aeruginosa*.

[15]Correspondence: daniel.hassett@uc.edu

Introduction

Morphologic data suggests that the airway lumen of cystic fibrosis (CF) patients harbor *Pseudomonas aeruginosa* biofilms that are characterized as spherical microcolonies (Costerton et al., 1981). The biochemical and genetic mechanisms utilized by *P. aeruginosa* to form biofilms have recently been elucidated in vitro with aerobic flow-through systems, which have emphasized the role of quorum-sensing (QS) pathways. Recent chemical studies revealed that CF sputum contains two QS signaling molecules, *N*-butyryl-L-homoserine lactone (C_4-HSL) and *N*-(3-oxododecanoyl)-L-homoserine lactone (3O-C_{12}-HSL), at a 3:1 ratio of C_4-HSL to 3O-C_{12}-HSL (Singh et al., 2000). Both molecules participate in QS signaling processes that involve two master transcriptional activator pairs, LasR/3O-C_{12}-HSL and RhlR/C_4-HSL, respectively. The in vitro formation of aerobic *P. aeruginosa* biofilms on abiotic substrata is dependent, in part, upon the LasR/3O-C_{12}-HSL QS system (Davies et al., 1998) and the presence of flagella and type IV pili (O'Toole and Kolter, 1998).

In contrast to aerobic in vitro biofilms, *P. aeruginosa* biofilms in the CF lung grow in stagnant mucus, and recent data have revealed that this environment is anaerobic and favors production of the viscous exopolysaccharide, alginate (Worlitzsch et al., 2002). *P. aeruginosa* is also capable of planktonic (detached) growth via anaerobic or aerobic respiration. Nitrate (NO_3^-), nitrite (NO_2^-), and nitrous oxide (N_2O) are terminal electron acceptors that support anaerobic respiration. The sequential eight-electron reduction of NO_3^- to N_2 is also called denitrification. Sufficient NO_3^- has been measured in CF airway surface liquid (Worlitzsch et al., 2002) and CF sputum (Hassett, 1996; Jones et al., 2000) to permit growth of *P. aeruginosa* under anaerobic planktonic conditions.

In this study, we explored the hypothesis that CF airways may be infected by a heretofore undescribed form of *P. aeruginosa* biofilms, i.e., those that develop and persist under static, anaerobic conditions. We first performed in vitro experiments to test whether *P. aeruginosa* could form biofilms under such conditions. Next,

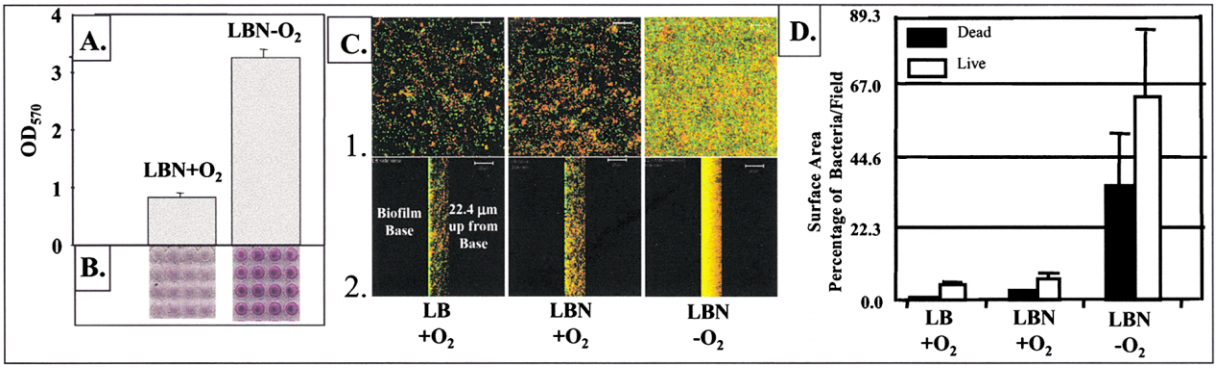

Figure 1. Influence of Oxygen on *P. aeruginosa* Biofilm Formation

(A) Quantitative differences between aerobic and anaerobic biofilms after crystal violet solubilization with ethanol. Bars represent the x ± SEM of the crystal violet optical density at 570 nm (n = 16 wells).

(B) An overnight culture of wild-type *P. aeruginosa* PAO1 (~2×10^7 cfu) was used to inoculate LBN under aerobic or anaerobic conditions in microtiter dishes. Following incubation at 37°C for 24 hr, biofilms were stained with 1% crystal violet and photographed.

(C) Confocal laser microscopic analysis of aerobic and anaerobic *P. aeruginosa* PAO1 biofilms. Live cells are stained with syto-9 (green), and dead cells are stained with propidium iodide (red). The top (1) and sagittal views (2) are projected from a stack of 56 images taken at 0.4 μm intervals for a total of 22.4 μm. LB, L-broth; LBN, L-broth with 1% KNO_3.

(D) Quantification of biofilm cell viability. The *y* axis of the graph measures the proportion of the microscope field occupied by live (white bars) versus dead (black bars) bacteria. Six fields were measured and expressed as mean and standard deviation.

we explored pathways that allowed *P. aeruginosa* to adapt and survive as anaerobic biofilms, including whether bacterial products specific to anaerobic biofilms could be detected via proteomic analyses. Finally, we sought evidence from (1) analyses of secretions harvested from excised CF lungs and (2) CF patient humoral antibody responses that protein products important for anaerobic biofilm growth could be detected in vivo. Characterization of anaerobic biofilms may permit development of antimicrobial agents to combat CF airway disease with greater efficacy than those currently available.

Results

Robust *P. aeruginosa* Biofilm Formation during Anaerobic Versus Aerobic Conditions

First, we asked whether *P. aeruginosa* could form biofilms under strict anaerobic conditions. The conditions selected for this study mimic the static growth mode characteristic of biofilms in immobile mucus plaques within CF airways and contrast the "flow" biofilms, which better represent urinary tract, bloodstream, or catheter biofilm models. We first employed a simple, highly reproducible microtiter dish biofilm assay (O'Toole and Kolter, 1998) to assess whether (1) *P. aeruginosa* could form biofilms under strict anaerobic versus aerobic conditions and (2) how these biofilms differ, using parameters that included thickness, density, and viability. As shown in Figures 1A and 1B, *P. aeruginosa* biofilms formed during anaerobic growth were greater than 3-fold larger (i.e., more bacteria) than during aerobic conditions. Next, to determine the spatial architecture of anaerobic versus aerobic biofilms, we grew biofilms on circular glass coverslips and visualized them by confocal laser scanning microscopy, both from top to bottom and sagittal views. As shown in Figure 1C, aerobic biofilms (LB, $+O_2$) were characterized by typical microcolony formation, with more bacteria at the biofilm base. The addition of NO_3^- to the culture media stimulated slightly more bacteria to adhere to the glass surface and, again, the biofilm bacteria to be more concentrated at the base (LBN, $+O_2$). In contrast, a thick, compact biofilm was formed by anaerobic bacteria (LBN, $-O_2$). Using a vital stain and confocal microscopy, we observed that anaerobic biofilms contained ~1.8-fold greater live (green) versus dead (red) organisms, a trait similar to that in aerobic biofilms (Figure 1D). Despite the fact that anaerobic biofilms on glass were greater than when grown on plastic (~7- versus 3-fold; compare Figures 1C and 1D with 1A and 1B), our results confirm that *P. aeruginosa* prefers the anaerobic biofilm mode of growth.

Which Gene Products Are Required for Anaerobic, as Compared with Aerobic, Biofilms?

Because *P. aeruginosa* appears to be growing as anaerobic biofilms in CF airways (Worlitzsch et al., 2002), we compared selected gene products required for aerobic biofilms with those required for optimal anaerobic biofilm formation. As a reminder (Figure 2A), anaerobic respiration in *P. aeruginosa* (also called respiratory NO_3^- reduction, or denitrification) involves the sequential eight-electron reduction of NO_3^- to N_2. In contrast, assimilatory NO_3^- reduction involves uptake of NO_3^- and its reduction to NH_3. Also, recall that the in vitro formation of aerobic *P. aeruginosa* biofilms with aerobic flow-through systems is dependent, in part, upon the LasR/3O-C_{12}-HSL QS tandem (Davies et al., 1998) and the presence of flagella and type IV pili (O'Toole and Kolter, 1998). To test whether these gene products are required for anaerobic biofilm formation under static conditions, we grew wild-type and isogenic *lasR*, *rhlR*, *lasRrhlR*, *pilA* (pilus-deficient), and *fliC* (flagellum-deficient) mutants under aerobic versus anaerobic conditions. As shown in Figures 2B and 2C, the *lasR*, *rhlR*, *lasRrhlR*, and *pilA*

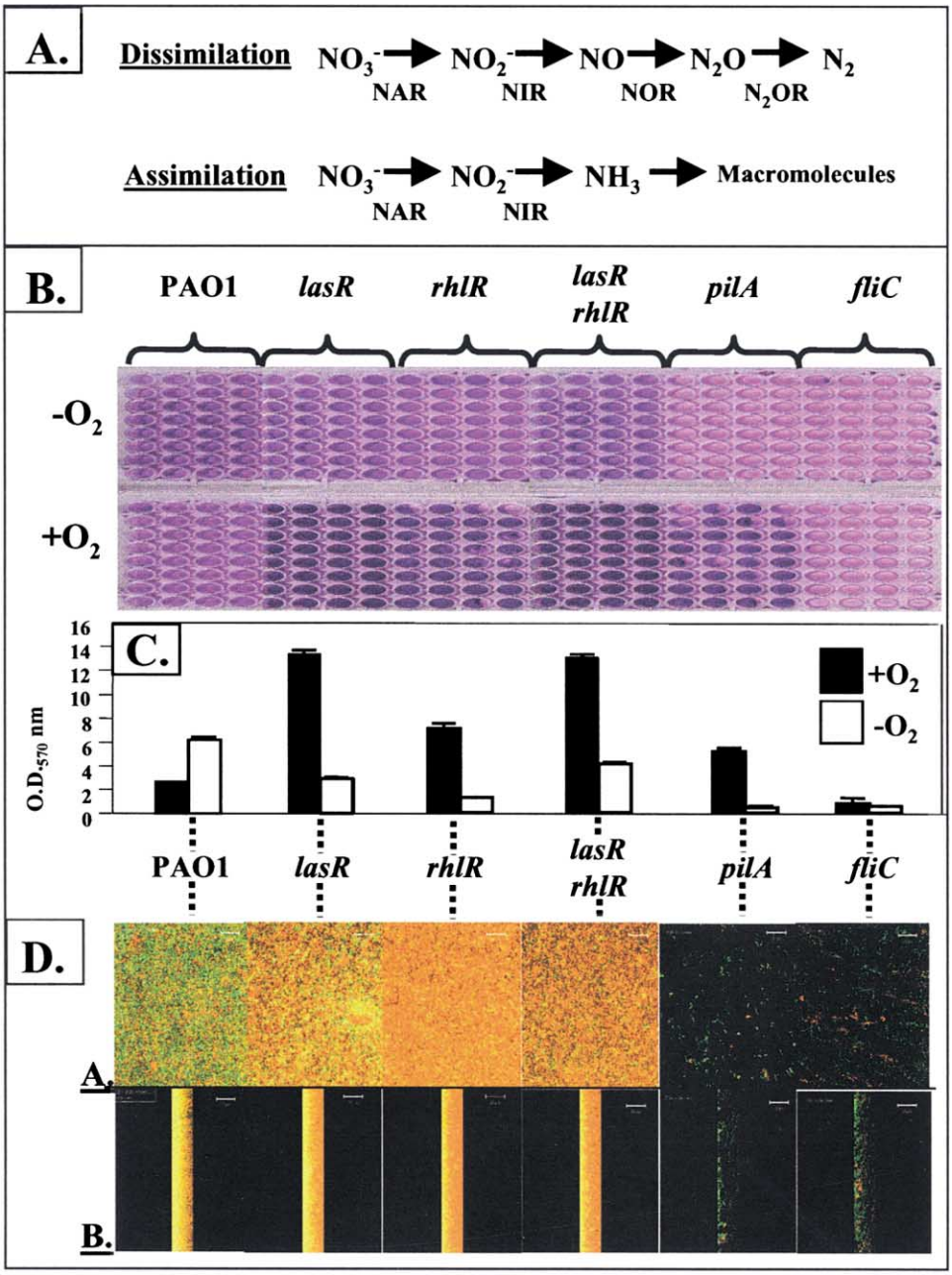

Figure 2. Influence of Oxygen on Biofilm Formation by Isogenic *P. aeruginosa* Mutants Known to Be Defective in Aerobic Biofilm Formation

(A) *P. aeruginosa* pathways for dissimilatory and assimilatory nitrate reduction. NAR, nitrate reductase; NIR, nitrite reductase; NOR, nitric oxide reductase; N_2OR, nitrous oxide reductase.

(B) Crystal violet staining of wild-type and isogenic mutants of *P. aeruginosa* grown as biofilms under aerobic ($+O_2$) or anaerobic ($-O_2$) conditions in LBN.

(C) Quantitative differences between aerobic (black bars) and anaerobic (white bars) biofilms.

(D) Confocal laser microscopic analysis of anaerobic *P. aeruginosa* biofilms. Genotypes are given above or between each panel or panel set. A, top view; B, sagittal view.

mutants formed very robust biofilms under aerobic conditions, even better than did wild-type bacteria. In contrast, none of the mutants could form anaerobic biofilms as well as did the wild-type bacteria. The *fliC* mutant produced poor biofilms, regardless of whether or not oxygen was present. This likely occurred because twitching motility, mediated by type IV pili, was reduced significantly in the *fliC* mutant during aerobic growth in the presence of NO_3^- and absent during anaerobic growth (data not shown). Consistent with this observation, one of the mutants revealed a pathway that was absolutely required for anaerobic biofilm formation. The

pilA mutant could form a good aerobic biofilm, presumably mediated by flagella, but formed poor anaerobic biofilms, suggesting that type IV pili are critical for anaerobic biofilm formation.

Gene Products Essential for Optimal Viability in Anaerobic Biofilms

Next, we examined the roles of LasR, RhlR, type IV pili, and flagella on anaerobic biofilm formation and cell viability on glass coverslips using confocal laser scanning microscopy (Figure 2D, parts A [top view] and B, [sagittal view]). Consistent with the results discussed above, isogenic *pilA* and *fliC* mutants formed very poor anaerobic biofilms relative to that formed by wild-type bacteria. In contrast, *lasR*, *rhlR*, and *lasRrhlR* mutants formed good biofilms, but the number of dead bacteria increased significantly in these mutants. Specifically, under anaerobic biofilm conditions, *lasR* and, to a greater extent, *rhlR* and *lasRrhlR* mutants were nearly all dead when evaluated by confocal laser quantification from the base (~20%–30% alive) to the top of the biofilm (~99% dead). Because impairment of QS leads to a rapid killing of anaerobic biofilm bacteria, we next pursued experiments designed to elucidate the mechanism of premature cell death.

Death of Anaerobic QS Mutants in a Biofilm Is Due to Metabolic Intoxication by Nitric Oxide (NO)

During denitrification, *P. aeruginosa* produces three gases, including NO, N_2O (nitrous oxide), and N_2 (nitrogen gas), with NO being a powerful antimicrobial agent (Fang, 1997). We hypothesized that death of *lasR*, *rhlR*, and *lasRrhlR* mutants in anaerobic biofilms reflected the relative concentration of NO produced by these organisms. To test this notion, a series of complimentary assays were employed. First, when the *rhlR* mutant was grown anaerobically in a biofilm, most bacteria were dead, except for some viable organisms (~20%) that were attached to the biofilm base (Figure 3A, panel 1). This result is consistent with the anaerobic *rhlR* mutant biofilm viability data provided in Figure 2D. The addition of 5 mM carboxy-PTIO, a stable nitroxide and potent scavenger of NO (Pfeiffer et al., 1997), protected the *rhlR* mutant (Figure 3A, compare panel 2 with panel 1). The protection conferred by carboxy-PTIO was observed primarily within the top 10–15 μm of the biofilm (Figure 3B, compare line 2 with line 1), a phenomenon likely due to the metabolism of this scavenger by bacteria at the biofilm base.

An indirect measure of NO is a decrease in aconitase activity (Kennedy et al., 1997). NO inactivates aconitase by nitrozation of the $[4Fe\text{-}4S]^{2+}$ center. As shown in Figure 3C, aconitase activity in the *rhlR* mutant was reduced ~50% relative to that in wild-type bacteria. Formation of a nitrosyl complex, such as Fe-S-NO, that is detectable by electron paramagnetic resonance spectroscopy is indicative of NO binding to the solvent-exposed iron of proteins with $[4Fe\text{-}4S]^{2+}$ centers (Kennedy et al., 1997). In the *rhlR* mutant, an NO-mediated iron-nitrosyl free radical spectrum was visible (Figure 3D, arrows), while a similar spectrum was absent in wild-type bacteria, indicating poisoning of proteins containing Fe-S centers.

To further examine the role of NO in anaerobic biofilm formation and cell viability, we grew biofilms in LBN under anaerobic conditions using a panel of mutant strains designed to test genetically whether NO killed the *rhlR* mutant bacteria. Figure 3E shows that most of the anaerobic Δ*rhlR* biofilm bacteria were dead, consistent with the results described above. In contrast, the majority of the *rhlRnirS* double mutants, which lack the only enzyme that produces NO (nitrite reductase) in *P. aeruginosa*, were alive. In addition, other mutants deficient in nitrite reductase RpoN (a sigma factor that controls *nirS* expression) and a double *rhlRrpoN* mutant were also alive. In parallel, a *norCB* mutant generated virtually no biofilm under anaerobic conditions, likely because the NO produced during anaerobic growth could not be detoxified, leading to very poor cell growth. A mutant deficient in the blue copper electron carrier azurin (*azu*) was also tested in this study. Because azurin feeds electrons to NO_2^- reductase, the *azu* mutant should not overproduce NO. Consistent with our focus for a role of NO in this toxicity, the *azu* mutant formed a robust, viable biofilm during anaerobic growth.

Finally, to assess whether enhanced NO production in the *rhlR* mutant was directly attributable to a dysregulation of denitrifying enzyme activities, NO_3^-, NO_2^-, and NO reductase activities were assayed in anaerobic cell extracts of selected strains. NO_3^- reductase (NAR) was increased >5-fold in the *rhlR* mutant (lane 2) and 4-fold in the *rhlRrpoN* mutant (lane 3) relative to that in wild-type bacteria (Figure 3F, lane 1). Moreover, NO_2^- reductase (NIR, converting NO_2^- to toxic NO) activity of the *rhlR* mutant (lane 2) was nearly 7-fold that of wild-type bacteria (lane 1), but only 1.5-fold higher in *rhlRrpoN* (lane 3). The NIR activity detected in the *rhlRrpoN* mutant suggests that the lack of *rhlR* plays a role in *nirS* activation that is RpoN independent. The *nirS* mutant (lane 4) produced negligible NIR activity. In contrast to the marked increases in NAR and NIR activity of the *rhlR* mutant, protective NO reductase (NOR) activity of the *rhlR* mutant (lane 2) was only 2-fold that of wild-type organisms (lane 1). In contrast, NOR activity in the *rhlRrpoN* (lane 3) and *nirS* mutant (lane 4), which have little or no NIR activity, was reduced ~30% relative to the activity in wild-type. Collectively, the data in Figure 3 demonstrate that dysregulation of anaerobic NO_3^- respiration in the *rhlR* mutant, leading to overproduction of NO, is the cause of premature cell death in these organisms. In contrast, anaerobic organisms lacking or possessing reduced NIR activity, such as *nirS*, *rpoN*, or *azu* mutants, thrive under such conditions.

Aerobic Versus Anaerobic Biofilm Proteomics: A Link Found to Differences in Overall Biofilm Physiology

Because biofilm formation during anaerobic growth was more robust than under aerobic conditions, we next asked whether there were proteins expressed that supported the anaerobic biofilm mode of growth. To test this notion, we grew whole-cell lysates from biofilm bacteria in LBN under aerobic and anaerobic conditions and separated them by 2D gel electrophoresis (Figures 4A [aerobic] and 4B [anaerobic]). A total of 240 protein spots were detected in the anaerobic biofilm gel with

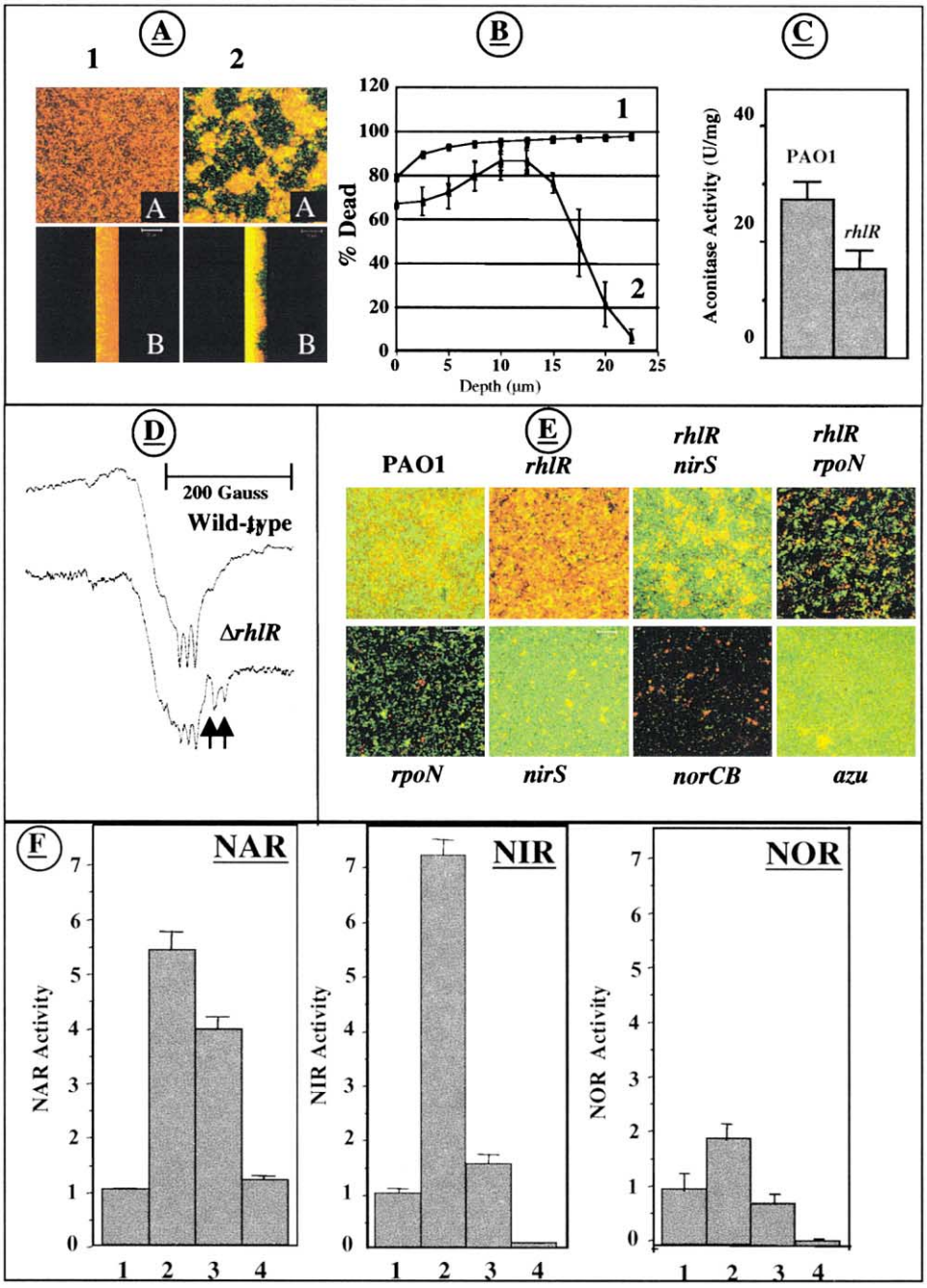

Figure 3. Overproduction of NO by Δ*rhlR* Bacteria Accounts for Anaerobic Cell Death

(A) *P. aeruginosa rhlR* mutant bacteria were grown as biofilms under anaerobic conditions, as described in Figure 2D, and top and sagittal images were captured by scanning confocal laser scanning microscopy. Panels 1A and 1B, Δ*rhlR*; panels 2A and 2B, Δ*rhlR* plus 5 mM carboxy-PTIO.

(B) Quantitative assessment of biofilm viability from the sagittal sectioning data gleaned in panels 1 and 2. Line 1, Δ*rhlR*; line 2, Δ*rhlR* plus 5 mM carboxy-PTIO.

(C) Anaerobic aconitase activity (x ± SEM, n = 3).

(D) EPR spectra of anaerobic PAO1 and Δ*rhlR* bacteria. The arrows denote the NO-Fe-S cluster signals in *rhlR* mutant bacteria.

(E) Anaerobic biofilms were grown, and top view confocal images were collected. The strain designation is given above or below each panel.

(F) NO_3^- (NAR), NO_2^- (NIR), and NO (NOR) reductase activity in stationary phase cell extracts of anaerobically grown bacteria. The relative level of wild-type NAR, NIR, and NOR activity was assigned a value of 1 and used as a comparison with activities of various test strains. Lane 1, PAO1; lane 2, *rhlR*; lane 3, *rhlRrpoN*; lane 4, *nirS*.

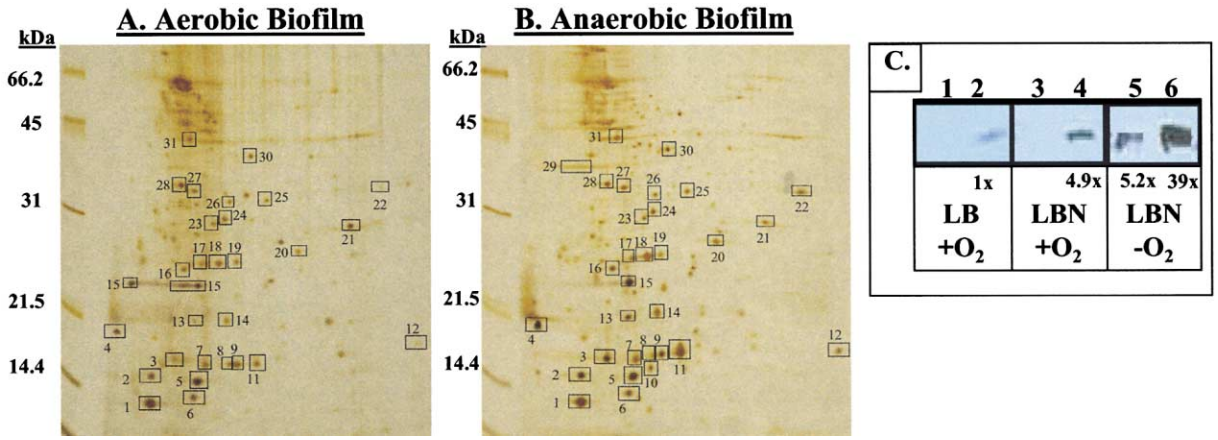

Figure 4. Two-Dimensional SDS Polyacrylamide Gel of Aerobic and Anaerobic Biofilm *P. aeruginosa* Proteins

P. aeruginosa PAO1 was grown in microtiter dishes containing aerobic LBN (A) or anaerobic LBN (B) for 24 hr at 37°C. Biofilm bacteria were harvested at 4°C and were poured over crushed ice to prevent new protein synthesis. Whole-cell extracts from aerobic and anaerobic biofilm samples were separated via 2D gel electrophoresis and stained with silver nitrate. The relative intensity of boxed spots in each 2D gel was quantified by Melanie 3.0 2D imaging software (see Table 1).

(C) Relative abundance of OprF in three different in vitro cultures; aerobic L-broth biofilm (lanes 1 and 2), aerobic LBN biofilm (lanes 3 and 4), anaerobic LBN biofilm (lanes 5 and 6). Lanes 1, 3, and 5 contain 0.5 μg protein. Lanes 2, 4, and 6 contain 5 μg protein. Lane 2 served as the aerobic control for quantification, a value set at 1X.

the default parameter setting and Melanie 3.0 software, while 213 protein spots were detected in the aerobic biofilm gel. Thirty-one spots from identical locations were excised from these gels, and 26 proteins were identified by MALDI-TOF analyses. The proteins are listed in Table 1, with their relative expression levels under each condition (Table 1, Quantification). Of the 31 protein spots excised for analysis, ~77% showed greater expression during the anaerobic biofilm mode of growth. The iron-cofactored superoxide dismutase (PA4366) was expressed equally under aerobic and anaerobic conditions. Curiously, there was only one protein that revealed a modest, yet reproducible, 1.8-fold increase in expression in aerobic, relative to anaerobic, biofilms. This was TonB, a protein important in iron sensing/acquisition (Takase et al., 2000). Because aerobic biofilms can have anaerobic zones, one interpretation of this finding is that aerobic biofilms contain a mixture of aerobic and anaerobic bacteria, consistent with a previous report (Ventullo and Rowe, 1982). The most highly expressed anaerobic biofilm protein was azurin, which was produced at 5.3-fold greater levels than it was in aerobic biofilms. Third, and most importantly, two proteins were detected only in anaerobic biofilms. One was the 50S ribosomal protein L9, the expression of which allowed for two forms. Under aerobic and anaerobic conditions, the protein was nearly equally represented by a 15.5 kDa form. However, a smaller form (spot 10) was observed only under anaerobic conditions. Interestingly, the second protein detected only in anaerobic biofilms was OprF, a channel-forming porin that has been shown to be involved in cell shape and growth in a low-salt environment (Rawling et al., 1998).

Because OprF has been reported to be constitutively produced by *P. aeruginosa* (Price et al., 2001), we next quantified the level of OprF expression in aerobic versus anaerobic biofilms by a Western blot analysis. Figure 4C shows that OprF expression was increased 4.9-fold during aerobic biofilm growth with NO_3^- (lane 4 versus lane 2). In contrast, OprF expression was dramatically (39-fold) upregulated during anaerobic biofilm growth (Figure 4C, lanes 5 and 6). Thus, the relative abundance of OprF expressed during anaerobic biofilm growth explains why it was not detected in aerobic biofilm 2D gels in the presence of NO_3^-.

CF Patients with Chronic *P. aeruginosa* Infections Have Lung Secretions Harboring, and Raise Antibodies to, OprF

Because OprF may be important for anaerobic biofilm formation, we next tested whether OprF is expressed in vivo during chronic CF airway disease. We used analyses that (1) link OprF expression directly to our in vitro data and (2) supplement these data with important evidence that OprF antibodies are raised by CF patients who are chronically infected with *P. aeruginosa*. First, to assess whether OprF is produced in CF patients, a Western analysis was performed with the membrane fraction of airway secretions harvested from a lung resected from a chronically infected CF transplant patient with a bacterial density in airway mucus of ~10^7–10^8 cfu/ml. Figure 5A (lanes 1–3) shows that secretions contained a cleaved, ~20 kDa OprF crossreactive protein. The normal size of OprF is 35 kDa, yet papain or trypsin cleavage results in a 20 kDa fragment containing the N-terminal half of OprF, which forms a protease-resistant β barrel that contributes to the transmembrane pore (Brinkman et al., 2000). As a control, this fragment from the in vivo specimen crossreacted with a monoclonal antibody derived from an N-terminal linear OprF peptide (Figure 5B, lane 3), but not with a C-terminal antibody (lane 6). As controls, both antibodies crossreacted with wild-type (Figure 5B, lanes 1 and 4), but not *oprF*, mutant cell extracts (Figure 5B, lanes 2 and 5). Thus, although expression of OprF in secretions is lower than in in vitro-grown anaerobic biofilms (~10^9 cfu/ml), the amount of *P. aeruginosa* in secretions is estimated to be 1–2 logs

Table 1. Analyses of *P. aeruginosa* Proteins for Identification and Quantification

Spot Number	Protein Name	PA Number	Z Value	MW	pI	Quantification ($+O_2/-O_2$)
1						1568/1625
2	Thioredoxin	PA5240	1.72	12	4.7	478/742
3	Probable DNA binding stress protein	PA0962	1.88	18.4	5	253/667
4	Hypothetical 18.6 kDa protein	AAK15336[a]	1.97	18.6	4.4	448/971
5	GroES chaperonine	PA2021	1.65	10.3	5.2	1038/1116
6	ATP synthase epsilon chain	PA5553	1.83	14.7	5.1	505/610
7						501/655
8	50S ribosomal protein L9	PA4932	2.39	15.5	5.4	261/210
9	Nucleoside diphosphate kinase	PA3807	2.32	15.6	5.5	512/542
10	50S ribosomal protein L9	PA4932	2.25	15.5	5.4	ND/340
11	Azurin precursor	PA4922	1.4	16.1	6.4	374/1972
12	50S ribosomal protein L10	PA4272	1.69	17.6	8.9	138/350
13	Probable thiol peroxidase	PA2532	1.9	17.4	5.2	184/420
14	Conserved hypothetical protein	PA3309	2.36	16.5	5.5	266/689
15	Fe cofactored superoxide dismutase	PA4366	2.34	21.9	5.3	995/986
16	Inorganic pyrophosphatase	PA4031	2.21	19.4	5	306/412
17	Probable peroxidase	PA3529	2.1	21.9	5.4	264/332
18	Probable peroxidase	PA3529	2.33	21.9	5.4	449/1026
19						259/202
20	Alkyl hydroperoxide reductase (AhpC)	PA0139	1.91	21.6	5.9	209/377
21	Probable TonB-dependent receptor	PA5505	2.39	28.1	7.9	423/236
22	Probable binding protein component of ABC	PA1342	2.09	35.2	8.5	91/248
23	Arginine/ornithine binding protein AotJ	PA0888	2.37	29	6.6	230/197
24	Hypothetical protein	PA4495	2.14	25.1	5.8	328/302
25						138/233
26						187/179
27	Elongation factor Ts	PA3655	1.76	30.7	5.2	232/413
28	Electron transfer flavoprotein alpha subunit	PA2951	2.01	32.3	5	487/387
29	Outer membrane protein OprF	PA1777	1.71	38.8	5	ND/196
30	Alcohol dehydrogenase	PA5427	2.22	36.3	5.6	233/258
31	Branched chain amino acid transport	PA1074	1.86	40.1	5.6	315/423

Thirty-one reproducibly represented proteins containing at least 1 pmol of protein were selected for mass spectrometric analysis. Twenty-six proteins were identified with significant certainty (Z value > 1.2) and are listed with their PA numbers. pI values and molecular weights are given in kilodaltons. Spot intensities were measured and normalized as described in Experimental Procedures. Each quantification value has an arbitrary unit provided by the Melanie 3.0 software. The first values indicate protein expression during aerobic biofilm growth, and the second values indicate protein expression during anaerobic biofilm growth. All spots that show increased expression in anaerobic biofilms are underlined.

[a] A GenBank accession number was assigned to this protein, because no PA number is available for this protein in the *P. aeruginosa* genome database (http://www.pseudomonas.com).

less. Thus, expression of OprF in vivo is consistent with that of anaerobic biofilm expression in vitro.

Next, we focused our Western analyses on antibodies to OprF using sera from a broad spectrum of CF versus normal individuals (Figure 5C). Our hypothesis was that chronically infected CF patients harboring anaerobically growing *P. aeruginosa* would raise OprF antibodies. Only chronically infected CF patients with $>10^6$ *P. aeruginosa*/ml sputum raised antibodies to OprF (lanes 13–17). Normals (lanes 1–3), a normal with *P. aeruginosa* pneumonia (lane 4), the corresponding author who has worked with *P. aeruginosa* for more than 11 years (lane 5), and CF patients that are sputum-negative for *P. aeruginosa* possessed no OprF antibodies.

Role of OprF in Anaerobic Growth and NO_2^- Reductase Activity

Because OprF is expressed in anaerobic in vitro biofilms and in CF airway mucus, we wished to determine whether OprF is required for anaerobic biofilm formation. Figure 6A shows that the *oprF* mutant formed a very poor biofilm relative to that formed by wild-type bacteria. To test whether this defect was a function of impaired anaerobic growth of the *oprF* mutant, we performed an anaerobic growth curve. Figure 6B demonstrates that the growth rate of the *oprF* mutant ($g = 2.34\ hr^{-1}$) was 1.8-fold slower than that of wild-type bacteria ($g = 1.3\ hr^{-1}$) and that the peak cell density was at least 40-fold less. During anaerobic growth, NO_3^- is taken up and released as NO_2^-, typically via NarK2-like extrusion pumps. Once NO_3^- is low, however, NO_2^- can be taken up for additional energy. Figure 6C demonstrates that NO_3^- uptake is more rapid in wild-type bacteria than in the *oprF* mutant. This suggests that OprF could be a channel for NO_3^-, NO_2^-, or both molecules, since each can be used as anaerobic terminal electron acceptors. In addition, although wild-type bacteria consumed NO_2^- to undetectable levels after 8 hr of growth, NO_2^- accumulated in the *oprF* mutant culture supernatants (Figure 6D). We then found that the *oprF* mutant lacked NIR activity (Figure 6E), but not NAR or NOR activities. This explains why (1) NO_2^- accumulated in the medium and (2) the *oprF* mutant cannot grow anaerobically using NO_2^- (data not shown). Still, the precise role of OprF in such processes is unknown. One postulate could be that OprF stabilizes NO_2^- activity. However, because OprF is known to associate with peptidoglycan, the lack of OprF would destabilize the

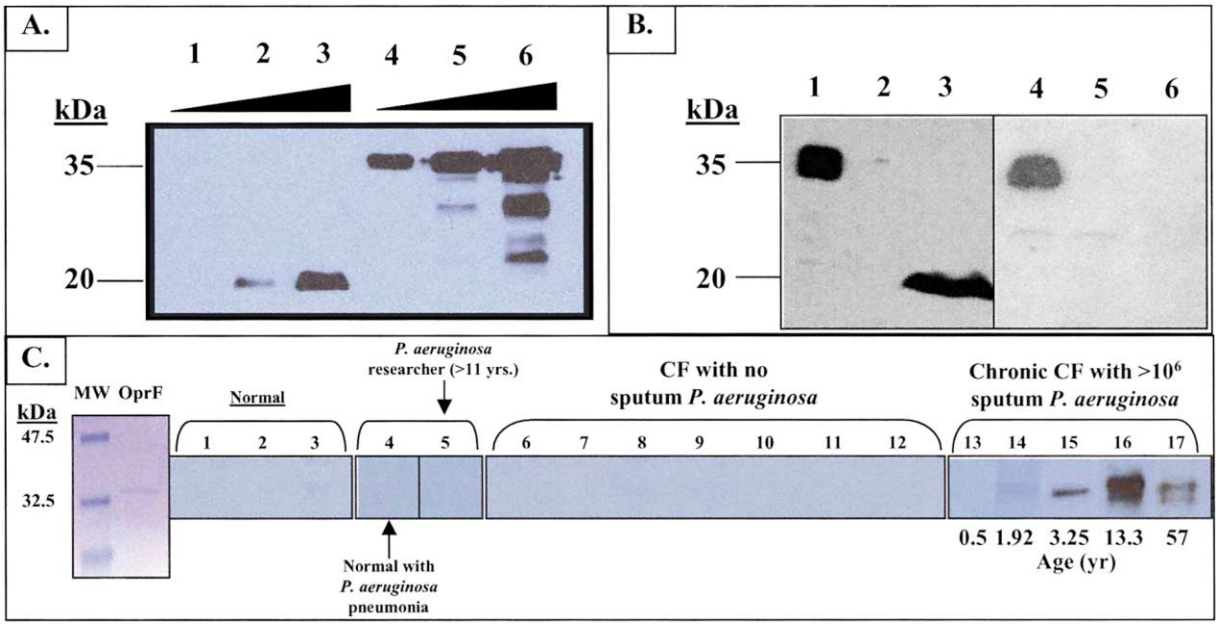

Figure 5. Identification of OprF in CF Lung Secretions and Production of Anti-OprF Antibodies by Chronically Infected CF Patients

(A) Comparison of OprF present in secretions from a chronically infected CF patient with the amount of OprF produced in anaerobically grown *P. aeruginosa*. Lanes 1–3, CF lung secretions from a chronically infected transplant patient; lanes 4–6, whole cell proteins from PAO1 grown anaerobically in LBN. Lanes 1 and 4, 100 ng; lanes 2 and 5, 1 μg; lanes 3 and 6, 10 μg.

(B) Western blot analysis of OprF production using wild-type (lanes 1 and 4), *oprF* mutant (lanes 2 and 5), and airway secretions (lanes 3 and 6). The antibody used for lanes 1–3 was derived against a linear N-terminal OprF epitope, while that used to probe lanes 4–6 was derived against a C-terminal epitope.

(C) Purified recombinant *P. aeruginosa* OprF was blotted onto PVDF membranes prior to western analysis with serum from normal patients, normal individuals with *P. aeruginosa* pneumonia, CF patients with no sputum *P. aeruginosa*, or chronically infected CF patients with $>10^6$ sputum *P. aeruginosa*/ml. Sera from normal patients (lane 1, 0.83 years; lane 2, 2 years; lane 3, 2.25 years); sera from normal individuals with *P. aeruginosa* pneumonia (lane 4, 2.68 years with $>10^6$ *Staphylococcus aureus* and $>10^6$ *P. aeruginosa*; lane 5, corresponding author who has worked with *P. aeruginosa* over 11 years); sera from CF patients with no sputum *P. aeruginosa* (lane 6, 11.1 years; lane 7, 2.5 years with 10^5 *Hemophilus influenzae* and 10^3 *Streptococcus pneumoniae*; lane 8, 0.1 years with 2×10^3 airway oropharyngeal flora; lane 9, 3.75 years with 4×10^4 airway oropharyngeal flora; lane 10, 0.16 years with 4×10^3 airway oropharyngeal flora; lane 11, 3.5 years with 1×10^4 airway oropharyngeal flora; lane 12, 6.83 years with 1×10^3 airway oropharyngeal flora); sera from chronically infected CF patients with $>10^6$ *P. aeruginosa* in sputum (lane 13, 0.5 years with 5×10^6 *P. aeruginosa*; lane 14, 3.25 years with 1×10^6 *P. aeruginosa*; lane 15, unknown age with 2×10^7 *P. aeruginosa*; lane 16, 13.25 years with $>1 \times 10^6$ *P. aeruginosa*; lane 17, 57 years, ΔF508/R117H).

peptidoglycan layer, possibly allowing for leakage of periplasmic proteins, one of which is NIR.

Discussion

P. aeruginosa Prefers the Anaerobic Biofilm Mode of Growth

An initiating event in the pathogenesis of CF lung disease is mucus stasis (Matsui et al., 1998; Tarran et al., 2001). Recently, Worlitzsch et al. (2002) demonstrated that steep hypoxic gradients are present in stationary mucus plaques from CF airway cultures. Oxygen consumption by bacteria, neutrophils, and CF airway cells render the thick mucus essentially anaerobic, after the onset of bacterial infection. Consequently, the goals of this study were to (1) assess the capacity of *P. aeruginosa* to form and survive in anaerobic biofilms and (2) identify gene products specific to, and critical for, such processes. Information gleaned from such studies would permit testing of the relevance of the anaerobic biofilm concept to CF patients in vivo and, in the process, potentially identify clues for therapeutic intervention.

The *rhl* QS Circuit and Anaerobic *P. aeruginosa* Infections in CF Airway Disease

Recently, a 3:1 ratio of C_4-HSL to 3O-C_{12}-HSL has been measured in in vitro biofilms and in CF sputa (Singh et al., 2000). Thus, the RhlR-C_4-HSL tandem would be predicted to be important for survival of bacteria during anaerobic CF lung disease. Our studies show that bacteria lacking RhlR die via metabolic NO suicide because of 5- and 7-fold dysregulatory increases in NAR and NIR activities, respectively. The small increase (2-fold) in potentially protective NOR activity in the *rhlR* mutant cannot provide relief from such toxic NO levels. Thus, we believe that the *rhl* QS circuit and, in particular, critical components related to NO_3^--mediated anaerobic respiration could be targets for the killing of anaerobic biofilm *P. aeruginosa* in CF lung disease.

Other Mutations that Could Support Anaerobic Survival of *P. aeruginosa* in Chronically Infected CF Airways

In contrast to the rapid death of anaerobic *rhlR* mutant bacteria, anaerobic *rhlRnirS*, *rhlRrpoN*, *nirS*, *rpoN*, and

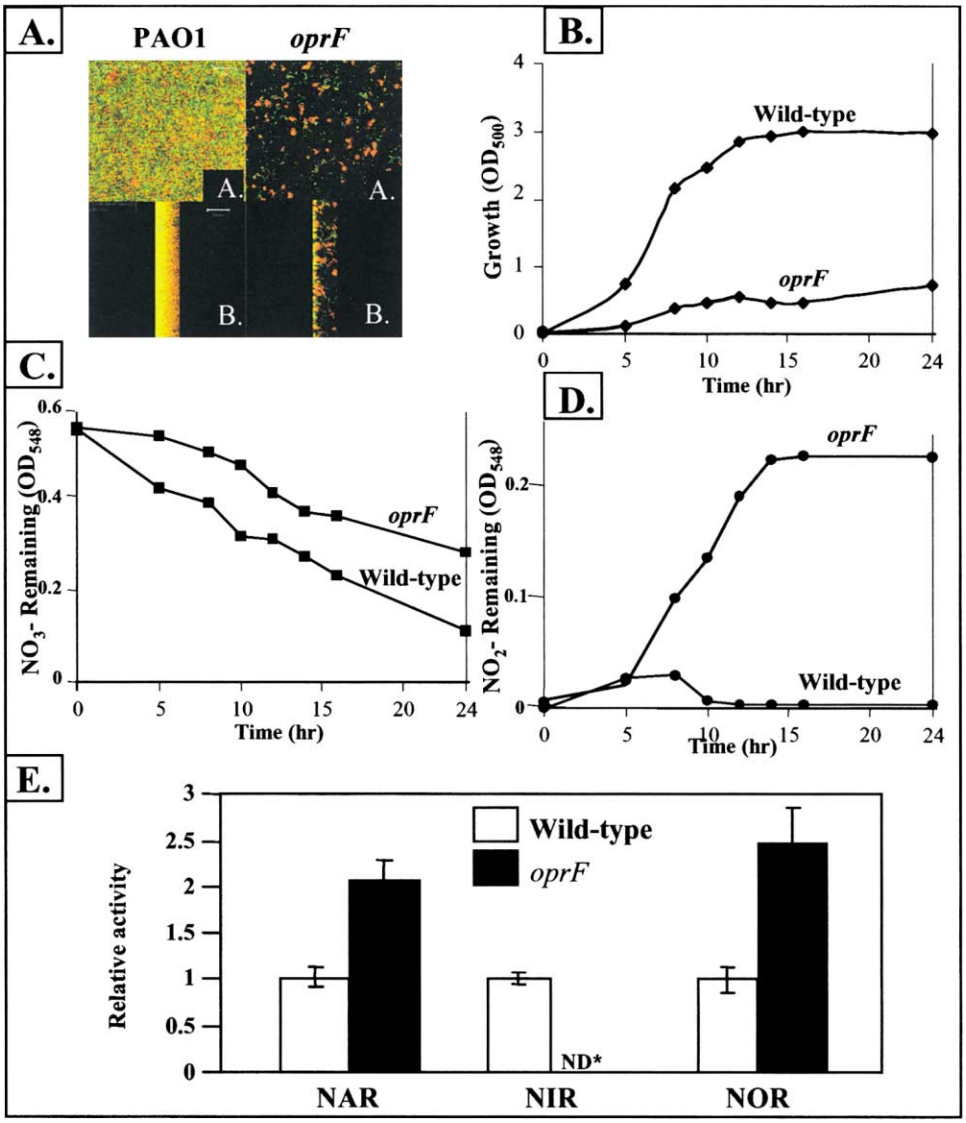

Figure 6. Role of *P. aeruginosa* OprF in Anaerobic Growth, Biofilm Formation, and Dissimilatory Nitrate Reduction

(A) Top and sagittal images of wild-type PAO1 and *oprF* mutant bacteria grown as anaerobic biofilms.

(B) Anaerobic growth curves of wild-type and *oprF* mutant bacteria.

(C) Nitrate uptake of wild-type and *oprF* mutant bacteria.

(D) Nitrite levels in culture media of wild-type and *oprF* mutant bacteria.

(E) Anaerobic NAR, NIR, and NOR activity in wild-type (white bars) and *oprF* mutant bacteria (black bars) (n = 3, x ± SEM). ND, not detected.

azu mutant biofilms were mostly alive. The unifying feature of each of these mutants is that they have little or no anaerobic NIR activity and thus generate low NO levels. Virtually all strains used in this study, with the exception of a *norCB* mutant, were capable of robust anaerobic growth with NO_3^- as a terminal electron acceptor. Thus, in the case of an *rhlR* mutant lacking NIR or RpoN, there is sufficient ATP production from NO_3^- reduction to NO_2^- without conversion to potentially toxic NO. In CF, sputum isolates frequently possess *rpoN* mutant phenotypes, including a lack of flagella and type IV pili (Mahenthiralingam et al., 1994). In fact, 39% of sputum isolates from 1030 chronically infected CF patients lacked flagella and pilus-mediated motility, and many were complemented by multiple copies of the *rpoN* gene (Mahenthiralingam et al., 1994). It was postulated that mutants lacking RpoN might have a survival advantage because they resist nonopsonic phagocytosis and also conserve energy. In addition, *rpoN* mutant bacteria produce markedly reduced NIR activity, which protects them from NO poisoning.

OprF, an Outer Membrane Protein Critical for Optimal Anaerobic Growth that Is also Produced in Abundance during Chronic CF Lung Disease

We found that the outer membrane porin, OprF, was only detectable in anaerobic biofilms on the basis of the sensitivity of 2D gels and MALDI-TOF proteomic identification technologies. Importantly, we also detected OprF in secretions harvested from freshly excised

lungs of CF patients. We also found that OprF antibodies are raised by CF patients that are chronically infected with *P. aeruginosa*, suggesting that OprF is constitutively expressed during the course of CF lung disease. The importance of OprF in anaerobic growth was revealed by the *oprF* mutant exhibiting a (1) dramatically impaired anaerobic growth rate and final cell density relative to those of wild-type bacteria and (2) complete absence of NIR activity. Although the precise mechanism connecting OprF to an absence of NIR activity is unknown, two potential scenarios could occur. First, because OprF has been shown to be associated with peptidoglycan (Rawling et al., 1998), a destabilized peptidoglycan in an *oprF* mutant might allow cells to be highly fragile. This, in turn, could lead to leakage of periplasmic proteins into the extracellular milieu. Yet this seems unlikely, since there would still be little or no NO_2^- in the supernatant. A more likely explanation is that OprF may interact directly with NIR, allowing for a stabilization of enzymatic activity.

Relatedly, CF lung disease is dramatically worsened when *P. aeruginosa* converts to the mucoid, alginate-overproducing form (Bayer et al., 1991). OprF has been detected in mucoid, but not in nonmucoid, bacteria (Malhotra et al., 2000), yet the precise connection between OprF and mucoidy was unclear until now. Note that, when mucoid bacteria are grown under static aerobic conditions, these organisms revert to a nonmucoid, antibiotic- and phagocyte-susceptible form. When grown anaerobically, this does not occur (Hassett, 1996). Increased OprF expression and persistence of mucoid *P. aeruginosa* in CF provide additional evidence that the mucus lining the airways, especially in chronically infected CF patients, is anaerobic. Importantly, the efficacy of many antibiotics, such as the "frontline" CF aminoglycoside, tobramycin, is significantly reduced or ineffective under anaerobic conditions. The discovery of impaired anaerobic growth, NO_3^- uptake, and an absence of NIR in the *oprF* mutant suggest that OprF may provide an opportunity for developing a successful therapeutic strategy for combating anaerobic *P. aeruginosa* biofilms in CF lung disease. Since OprF has been successfully used as protein and DNA vaccines in a mouse model of *P. aeruginosa* chronic lung infection (Price et al., 2001), it is likely that anti-OprF antibodies may offer some protection during early CF airway disease.

In conclusion, this study provides sound evidence that *P. aeruginosa* forms better biofilms during anaerobic growth. The most efficient form of this mode of growth requires proteins/enzymes that allow *P. aeruginosa* to (1) utilize NO_3^- and NO_2^- as terminal electron acceptors, (2) influence the activity/stability of denitrifying enzymes (OprF), and (3) modulate production (*rhl* QS system) and removal (NOR) of NO. Thus, we suggest that these pathways represent candidate targets for a novel suite of antimicrobials, founded on the proposal that successful treatment of the disease may require the disruption of anaerobic respiration within the anaerobic airway mucus.

Experimental Procedures

Bacteria

All bacteria were derivatives of *P. aeruginosa* PAO1 (Holloway, 1969). Allelic exchange was used for deletion or insertion mutagenesis. Bacteria were grown in either Luria-Bertani (L)-broth or L-broth containing 1% KNO_3 (LBN).

Growth of Biofilms

Microtiter Dish Method

Polystyrene microtiter dishes containing 100 μl of L-broth or LBN/well were inoculated with 5 μl of 10-fold-diluted and optical density-adjusted overnight culture, and plates were allowed to incubate at 37°C under aerobic and anaerobic conditions for 24 hr. Anaerobic growth was achieved in an anaerobic chamber (Forma). Crystal violet staining and quantification of biofilms were performed as previously described (O'Toole and Kolter, 1998).

Confocal Examination of Biofilms

For biofilm architecture examination, circular coverslips were glued to the bottom of 35 × 10 mm polystyrene tissue culture dishes with small holes in the base (Falcon). The plates were sterilized overnight by UV irradiation. Three milliliters of aerobic L-broth, aerobic LBN, or anaerobic LBN was inoculated with $\sim 10^7$ cfu of overnight L-broth-grown culture. After 24 hr at 37°C, biofilms were washed with saline and stained with 0.5 ml of a LIVE/DEAD *Bac*Light bacterial viability stain (Molecular Probes, Eugene, OR). Images were acquired on a Zeiss LSM 510 laser scanning confocal unit attached to an Axiovert microscope with a 63 × 1.4 NA oil immersion objective. For two color images, samples were scanned sequentially at 488 nm and 546 nm. Syto 9 (green fluorescence) was detected through a 505–530 nm bandpass filter, and propidium iodine (red fluorescence) was detected through a 560 nm longpass filter and presented in two channels of a 512- × 512-pixel, 8-bit image.

Construction of a *P. aeruginosa* Tryptic Library Database

All 5570 translated open reading frames from the *P. aeruginosa* genome (http://www.pseudomonas.com/maps/map1.htm) were downloaded into ProFound (http://prowl.rockefeller.edu/cgi-bin/ProFound), and a tryptic fragment library was assembled.

Experiments Designed to Monitor NO Overproduction during Anaerobic Growth of *rhlR* Mutant Bacteria

Anaerobic Biofilm Protection by 2-(4-Carboxyphenyl)-4,4,5,5-Tetramethylimidazoline-1-Oxyl-3-Oxide (Carboxy-PTIO)

Biofilms of *rhlR* mutant bacteria were grown anaerobically in the presence, versus absence, of 5 mM carboxy-PTIO (Molecular Probes, Eugene, OR), an NO scavenger.

Aconitase Activity as an Indirect Measure of NO Poisoning

Cell extracts from anaerobic bacteria were prepared and assayed for aconitase activity (Gardner and Fridovich, 1991).

Electron Paramagnetic Resonance Spectroscopy of the Dinitrosyl-Iron-Dithiol Complex after Anaerobic Growth of P. aeruginosa

Wild-type and *rhlR* bacteria were grown for 48 hr under anaerobic conditions with shaking at 100 rpm. Samples were concentrated 10-fold, and aliquots were removed for assessment of turbidity and total cell dry weight. Equivalent turbid slurries of each organism were drawn into 1 ml tuberculin syringes that were immersed in a dewer of liquid nitrogen. The tip of the frozen syringe was then cut off, and the slurry was allowed to partially thaw, so that the frozen contents could slide out freely into a new dewer of liquid nitrogen. The frozen bacterial slivers were placed into an EPR cuvette that was kept at −180°C by liquid helium. Disassembly of the [3Fe-4S] clusters of the inactive forms of *P. aeruginosa* proteins upon the anaerobic production of NO is accompanied by the formation of two characteristic Fe-S-NO species. These were examined spectroscopically with a Bruker EMX EPR. The EPR settings were as follows: 77 K, 20 mW, MA, 4.0, 2.6 TC.

NO_3 (NAR), NO_2 (NIR), and NO Reductase (NOR) Activity Assays

NAR activity was measured in cell extracts of stationary phase anaerobic LBN-grown bacteria (Lester and DeMoss, 1971). For NIR and NOR activity assays, the disappearance of NO_2^- and NO was followed with the Griess reagent (Nims, 1995) and an NO electrode (Gardner et al., 1998), respectively.

Two-Dimensional Gel Electrophoresis and MALDI-TOF Mass Spectrometric Protein Analyses

Bacteria were grown in microtiter dishes under aerobic and anaerobic conditions. After 24 hr at 37°C, planktonic bacteria were removed, and the saline-washed biofilms were detached by scraping the wells. Cell extracts were prepared from cultures harvested by

centrifugation at 10,000 × g for 5 min at 4°C. Bacteria were washed twice in 10 mM Tris-HCl (pH 8.0) and, after three freeze-thaw cycles, sonicated on ice. Cell debris was clarified by centrifugation at 13,000 × g for 10 min at 4°C. Protein was estimated by the method of Bradford (Bradford, 1976). Immobiline Drystrips (Amersham) were used for separation of proteins in the first dimension. The strips were equilibrated in SDS-PAGE buffer and separated by 12% SDS-PAGE in the second dimension. Mass spectrometric protein identification was performed as previously described (Shevchenko et al., 1996, and http://proteomics.uc.edu). Protein spots were excised from 2D silver-stained polyacrylamide gels (http://proteomics.uc.edu/ Silver%20Stain.htm). Quantification of protein spots in 2D gels was performed with Melanie 3.0 imaging software (Swiss Institute of Bioinformatics). Protein spots were digitized and quantified on a volume basis by mathematical integration of optical density over spot area.

Acknowledgments

We thank Dr. Paul Quinton for donation of his sera. Support was by NIH grant AI-40541 and Cystic Fibrosis Foundation New Technology grant (D.J.H).

Received: February 13, 2002
Revised: August 2, 2002

References

Bayer, A.S., Speert, D.P., Park, S., Tu, J., Witt, M., Nast, C.C., and Norman, D.C. (1991). Functional role of mucoid exopolysaccharide (alginate) in antibiotic-induced and polymorphonuclear leukocyte-mediated killing of *Pseudomonas aeruginosa*. Infect. Immun. *59*, 302–308.

Bradford, M.M. (1976). A rapid and sensitive method for the quantitation of microgram quantities of protein utilizing the principle of protein-dye binding. Anal. Biochem. *72*, 248–254.

Brinkman, F.S., Bains, M., and Hancock, R.E. (2000). The amino terminus of *Pseudomonas aeruginosa* outer membrane protein OprF forms channels in lipid bilayer membranes: correlation with a three-dimensional model. J. Bacteriol. *182*, 5251–5255.

Costerton, J.W., Irvin, R.T., and Chen, K.-J. (1981). The role of bacterial surface structures in pathogenesis. Crit. Rev. Microbiol. *8*, 303–338.

Davies, D.G., Parsek, M.R., Pearson, J.P., Iglewski, B.H., Costerton, J.W., and Greenberg, E.P. (1998). The involvement of cell-to-cell signals in the development of a bacterial biofilm. Science *280*, 295–298.

Fang, F.C. (1997). Perspective series: host/pathogen interactions. Mechanisms of nitric oxide-related antimicrobial activity. J. Clin. Invest. *99*, 2818–2825.

Gardner, P.R., and Fridovich, I. (1991). Superoxide sensitivity of the *Escherichia coli* aconitase. J. Biol. Chem. *266*, 19328–19333.

Gardner, P.R., Gardner, A.M., Martin, L.A., and Salzman, A.L. (1998). Nitric oxide dioxygenase: an enzymic function for flavohemoglobin. Proc. Natl. Acad. Sci. USA *95*, 10378–10383.

Hassett, D.J. (1996). Anaerobic production of alginate by *Pseudomonas aeruginosa*: alginate restricts diffusion of oxygen. J. Bacteriol. *178*, 7322–7325.

Holloway, B.W. (1969). Genetics of *Pseudomonas*. Bacteriol. Rev. *33*, 419–443.

Jones, K.L., Hegab, A.H., Hillman, B.C., Simpson, K.L., Jinkins, P.A., Grisham, M.B., Owens, M.W., Sato, E., and Robbins, R.A. (2000). Elevation of nitrotyrosine and nitrate concentrations in cystic fibrosis sputum. Pediatr. Pulmonol. *30*, 79–85.

Kennedy, M.C., Antholine, W.E., and Beinert, H. (1997). An EPR investigation of the products of the reaction of cytosolic and mitochondrial aconitases with nitric oxide. J. Biol. Chem. *272*, 20340–20347.

Lester, R.L., and DeMoss, J.A. (1971). Effects of molybdate and selenite on formate and nitrate metabolism in *Escherichia coli*. J. Bacteriol. *105*, 1006–1014.

Mahenthiralingam, E., Campbell, M.E., and Speert, D.P. (1994). Nonmotility and phagocytic resistance of *Pseudomonas aeruginosa* isolates from chronically colonized patients with cystic fibrosis. Infect. Immun. *62*, 596–605.

Malhotra, S., Silo-Suh, L.A., Mathee, K., and Ohman, D.E. (2000). Proteome analysis of the effect of mucoid conversion on global protein expression in *Pseudomonas aeruginosa* strain PAO1 shows induction of the disulfide bond isomerase, *dsbA*. J. Bacteriol. *182*, 6999–7006.

Matsui, H., Grubb, B.R., Tarran, R., Randell, S.H., Gatzy, J.T., Davis, C.W., and Boucher, R.C. (1998). Evidence for periciliary liquid layer depletion, not abnormal ion composition, in the pathogenesis of cystic fibrosis airways disease. Cell *95*, 1005–1015.

Nims, R.W. (1995). A companion to methods in enzymology. Methods *7*, 48–54.

O'Toole, G.A., and Kolter, R. (1998). Flagellar and twitching motility are necessary for *Pseudomonas aeruginosa* biofilm development. Mol. Microbiol. *30*, 295–304.

Pfeiffer, S., Leopold, E., Hemmens, B., Schmidt, K., Werner, E.R., and Mayer, B. (1997). Interference of carboxy-PTIO with nitric oxide- and peroxynitrite-mediated reactions. Free Radic. Biol. Med. *22*, 787–794.

Price, B.M., Galloway, D.R., Baker, N.R., Gilleland, L.B., Staczek, J., and Gilleland, H.E., Jr. (2001). Protection against *Pseudomonas aeruginosa* chronic lung infection in mice by genetic immunization against outer membrane protein F (OprF) of *P. aeruginosa*. Infect. Immun. *69*, 3510–3515.

Rawling, E.G., Brinkman, F.S., and Hancock, R.E. (1998). Roles of the carboxy-terminal half of *Pseudomonas aeruginosa* major outer membrane protein OprF in cell shape, growth in low-osmolarity medium, and peptidoglycan association. J. Bacteriol. *180*, 3556–3562.

Shevchenko, A., Jensen, O.N., Podtelejnikov, A.V., Sagliocco, F., Wilm, M., Vorm, O., Mortensen, P., Boucherie, H., and Mann, M. (1996). Linking genome and proteome by mass spectrometry: large-scale identification of yeast proteins from two dimensional gels. Proc. Natl. Acad. Sci. USA *93*, 14440–14445.

Singh, P.K., Schaefer, A.L., Parsek, M.R., Moninger, T.O., Welsh, M.J., and Greenberg, E.P. (2000). Quorum-sensing signals indicate that cystic fibrosis lungs are infected with bacterial biofilms. Nature *407*, 762–764.

Takase, H., Nitanai, H., Hoshino, K., and Otani, T. (2000). Requirement of the *Pseudomonas aeruginosa tonB* gene for high-affinity iron acquisition and infection. Infect. Immun. *68*, 4498–4504.

Tarran, R., Grubb, B.R., Gatzy, J.T., Davis, C.W., and Boucher, R.C. (2001). The relative roles of passive surface forces and active ion transport in the modulation of airway surface liquid volume and composition. J. Gen. Physiol. *118*, 223–236.

Ventullo, R.M., and Rowe, J.J. (1982). Denitrification potential of epilithic communities in zootic environments. Curr. Microbiol. *7*, 29–33.

Worlitzsch, D., Tarran, R., Ulrich, M., Schwab, U., Cekici, A., Meyer, K.C., Birrer, P., Bellon, G., Berger, J., Wei, T., et al. (2002). Reduced oxygen concentrations in airway mucus contribute to the early and late pathogenesis of *Pseudomonas aeruginosa* cystic fibrosis airway infection. J. Clin. Invest. *109*, 317–325.